Electron Mobility and Scattering Processes in AgBr at Low Temperatures*

DWIGHT C. BURNHAM,† FREDERICK C. BROWN, AND ROBERT S. KNOX‡
Department of Physics, University of Illinois, Urbana, Illinois

(Received April 28, 1960)

The Hall effect for electrons released by light in high-purity crystals of AgBr has been studied experimentally in the temperature range 4° to 120°K. The observed mobilities exceed 20 000 cm²/volt-sec at very low temperatures. The general features of the dependence of low-field Hall mobilility on temperature can be understood by comparison with standard theory. A nearly exponential dependence of mobility on $1/T$ is observed from 40° to 120°K, as predicted for scattering by optical vibrations of the lattice. The slope of the $(\log \mu)$ versus $1/T$ data agrees quite well with the Debye Θ for the longitudinal optical mode as deduced from reststrahlen data. Below 40°K the observed mobilities can be explained in terms of a combination of the effects of optical, acoustical and charged impurity scattering. The last process appears to dominate below 15°K. High-field effects are observed which can be explained by classical transport theory assuming a conduction band of standard from as well as isotropic scattering.

I. INTRODUCTION

ALTHOUGH the silver halides AgBr and AgCl are less polar than alkali halide crystals, they have far more ionic character than most compound semiconductors. This may be seen by computing the Szigeti factor $s=e^*/e$, which is sometimes used to indicate the relative importance of ionic binding.[1] From available data one obtains values of s equal to 0.78 and 0.73 for AgCl and AgBr, respectively. In the case of the more ionic alkali halides $s\simeq 0.8$, whereas in less polar crystals, such as ZnS, s is as low as 0.48.

Our interest in ionic crystals centers on the electronic properties and, in particular, upon the electron-lattice interaction. The mobility of a conduction electron in the silver halides at room temperature is low (of the order of 40 cm²/volt sec),[2] largely because electrons in ionic crystals are very strongly scattered by optical modes of lattice vibration. In addition to this scattering, a slowly moving electron is surrounded by a cloud of phonons which can move with the electron and which results in a slightly lower energy for the electron and a greater effective mass.[3] A measure of the number of optical phonons carried along by a slow electron is obtained by computing the coupling constant[4] α, given in terms of the longitudinal optical mode frequency of the lattice ω_l, and the static and high frequency dielectric constants. For the silver halides, α is of the order of 2 to 3, which indicates a moderate polaron effect amenable to treatment, at least at low temperature, by present mobility theory.[4–7]

The Hall mobility of photoelectrons in AgCl[8] and in KCl[9] increases to high values (6000 cm²/volt sec for AgCl at 6°K) as the temperature is lowered. The present paper describes low temperature Hall and photoconductivity measurements on AgBr. It has turned out to be particularly interesting to compare the results for AgCl and AgBr. The two crystals are very similar in most respects, except that the bromide has a somewhat lower optical mode frequency and a smaller band gap. As will be shown, electron mobilities in AgBr rise to values in excess of 20 000 cm²/volt sec at 6°K, making it possible to study magnetoresistance and other effects of high magnetic fields.

The experimental methods are briefly described in Sec. II. Results given in Sec. IIIA show that although holes are mobile in AgBr, transient photocurrents at low temperature arise primarily because of the drift of electrons. The results of low field Hall measurements are presented in IIIB, whereas high field effects are given in Sec. IIIC. The temperature dependence of the Hall mobility is analyzed according to various scattering mechanisms in Sec. IVA, which deals with low field effects only. A comparison of the results with polaron theory is given in IVB. Finally, the observed high field effects are considered theoretically in Sec. IVC.

II. EXPERIMENTAL METHODS

Special attention was given to preparation of the crystals for these experiments on AgBr. The starting material was made by precipitation in dilute solutions of very high grade $AgNO_3$[10] and redistilled high purity HBr. After vacuum freeze drying and capillary

* Research supported in part by U. S. Air Force Office of Scientific Research. Based on thesis submitted by one of the authors (D.C.B.) in partial fulfillment of requirements for Ph.D. degree, University of Illinois, Urbana, Illinois.

† Present address: Research Laboratories, Eastman Kodak Company, Rochester, New York.

‡ Present address: University of Rochester, Rochester, N. Y.

[1] See, e.g., M. Born and K. Huang, *Dynamical Theory of Crystal Lattices* (Oxford University Press, New York, 1954), p. 112.

[2] J. R. Haynes and W. L. Shockley, Phys. Rev. **82**, 935 (1951).

[3] The electron plus its associated lattice polarization is called a "polaron."

[4] H. Fröhlich, *Advances in Physics* edited by N. F. Mott (Taylor and Francis, Ltd., London, 1954), Vol. 3, p. 325; Vol. 5, p. 412 (1956).

[5] T. D. Lee, F. Low, and D. Pines, Phys. Rev. **90**, 297 (1953).

[6] F. Low and D. Pines, Phys. Rev. **98**, 414 (1955).

[7] T. D. Schultz, Phys. Rev. **116**, 526 (1959).

[8] K. Kobayashi and F. C. Brown, Phys. Rev. **113**, 507 (1959).

[9] F. C. Brown and N. Inchauspé, International Conference on Color Centers, Oregon State College, September, 1959 (unpublished).

[10] Special Product, X-491, silver nitrate, obtainable from Eastman Organic Chemicals, Rochester, New York.

filtering,[11,12] the material was multiply zone refined in high vacuum.[13] Some crystals were cut directly from the zone refined ingot, while others were regrown by the Bridgman technique, using quartz crucibles and high vacuum. Spectrographic analysis[14,15] of some of the samples indicated that only a few parts in 10^7 heavy metal impurities, chiefly iron, were present.

The spectral dependence of the photoconductivity in crystals of AgBr thus prepared was studied in a manner previously described for AgCl.[16] In measurements of this type, the crystal is cooled to low temperature in order to freeze out the motion of ionic defects. A collecting voltage is applied between plane-parallel electrodes, and the crystal is illuminated with a pulse of light. The charge induced on the electrodes is measured by a sensitive electrometer and can be expressed in terms of the number of photons absorbed during the light flash, the quantum efficiency, and the range (Schubweg) of each carrier before it is trapped or collected at the electrodes. By using a very small total amount of illumination, it is possible to carry out the measurements in the absence of appreciable space charge or polarization, even though the electrodes are blocking. Reversal of the collecting voltage allows one to separate the drift or electrons from the drift of holes (under conditions of strongly absorbed light). It is particularly important to determine the relative range of holes and electrons in order to interpret the photoconductive Hall experiments.

The Hall mobility for carriers released by light was observed down to 4°K, using the method and apparatus of reference 8. Here a modification of the Redfield technique[17] was employed, which overcomes many of the difficulties associated with the buildup of space charge and the low signal-to-noise characteristic of measurements on very high impedance samples. A brief description of the method will be given in order to present the observations.

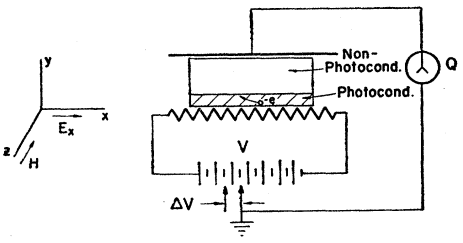

FIG. 1. Schematic diagram of the electrode arrangement for the Hall measurements. In practice the battery V is replaced by a low repetition rate pulse generator so that a negligible amount of power is dissipated in the resistance film at low temperature. The crystal is illuminated through the film with synchronized pulses of light from a spark light source. The detector Q is a low noise pre-amplifier and oscilloscope (see reference 8).

Figure 1 shows a crystal which is situated between plane parallel electrodes, one of which is a transparent resistance film, through which the crystal can be illuminated. The crystal is divided into two parts. The upper part (spacer) is either not illuminated or not photoconducting.[18] A current flows along the length of the resistance film and establishes an electric field, E_x, in the thin photoconducting part of the dielectric, predominantly in the x direction. This part of the dielectric is illuminated by a brief flash of light which releases photoelectrons that are free to drift in the applied field. An electrometer, or alternatively high gain amplifier, is connected as indicated in the figure, so as to measure the charge induced on the electrodes by a net flow of charge in the y direction. The measurement is a transient one carried out with single pulses at very low repetition rates. For the case where the electron drift range is short (neglecting saturation effects) and electrons only are assumed mobile, the induced charge is given by

$$Q=\int_{\text{Vol}} \frac{n_0 e v_y \tau_t}{D} d\mathbf{r}. \tag{1}$$

Here n_0 is the number of carriers released per unit volume by the light, v_y is the y component of drift velocity and τ_t is the mean time before trapping, and $e=-|e|$ is the charge of the electron. The thickness of the crystal is D and the integral extends over the illuminated volume of the crystal.[19]

If the position of the ground trap in Fig. 1 is adjusted carefully to correspond to the potential at the center of the resistance film, there is no *net* flow of charge in the y direction, and the electrometer records zero induced charge in the absence of a magnetic field. When a magnetic field is applied in the $-z$ direction, as shown, there will result a y component of drift velocity and a net charge Q will be induced on the electrodes following the brief flash of light. The amount of this charge can be expressed in terms of the applied electric and magnetic fields using Eq. (1) and $v_y=J_y/ne$ where J_y

[11] J. M. Hedges and J. W. Mitchell, Phil. Mag. 44, 357 (1953).
[12] F. C. Brown, J. Phys. Chem. Solids 4, 206 (1958).
[13] Details and results of the zone refining, carried out in cooperation with the group at Eastman Kodak Laboratories, will be presented elsewhere.
[14] N. R. Nail, F. Moser, P. E. Goddard, and F. Urbach, Rev. Sci. Instr. 28, 275 (1957).
[15] We are indebted to Dr. F. Urbach, Research Laboratories, Easterman Kodak Company, for conveying the results of the spectrographic analysis.
[16] R. S. Van Heyningen and F. C. Brown, Phys. Rev. 111, 462 (1958).
[17] A. G. Redfield, Phys. Rev. 94, 526 (1954); 94, 537 (1954).
[18] In the present case the photoconducting crystal was AgBr and the spacer AgCl. These two materials have nearly the same dielectric constant, but the absorption edge begins at longer wavelengths in AgBr. Light passes in turn through a thick AgBr filter (not shown in Fig. 1), the AgBr sample and finally the spacer. Absorption occurs throughout the volume of the sample but the long wavelength radiation which reaches the AgCl is not absorbed.
[19] The use of Eq. (1) and the development of the working equations in E and H which follow is justified by a more rigorous treatment, taking into account the fact that the electrons are not all released simultaneously, but that n may be a function of time. See D. C. Burnham, thesis, University of Illinois, 1959 (unpublished).

is the y component of equilibrium current density, $\mathbf{J}$, in the crystal.

To first order in electric field $\mathbf{E}$, the general form of $\mathbf{J}$ is (see Sec. IVC)

$$\mathbf{J}=\sigma(H)\mathbf{E}+\alpha(H)(\mathbf{E}\times\mathbf{H})+\gamma(H)(\mathbf{H}\cdot\mathbf{E})\mathbf{H}, \quad (2)$$

where $\mathbf{H}$ is the magnetic field and the coefficients σ, α, and γ are even functions of $\mu H/c$, where μ is the mobility and c the velocity of light. (These coefficients depend critically on the type of scattering mechanism and on the band structure.) Since $\mathbf{H}$ lies only along the z direction,

$$v_y=(1/n_0e)[\sigma(H)E_y-\alpha(H)E_xH]. \quad (3)$$

An electrical balance is obtained first for $H=0$, which assures that

$$Q(0)=\int_{\text{Vol}}\frac{\sigma(0)E_y\tau_t}{D}d\mathbf{r}=0. \quad (4)$$

Here $\sigma(0)$ is the value of the coefficient for zero magnetic field. Next, one measures Q as a function of H. Since H is uniform throughout the crystal and E_y is left unchanged $Q(H)$ is given by

$$Q(H)=\int_{\text{Vol}}[\sigma(H)E_y-\alpha(H)HE_x]\frac{\tau_t}{D}d\mathbf{r}$$

$$=-\frac{\tau_t}{D}\bar{E}_x\Omega\alpha(H)H, \quad (5)$$

where $\bar{E}_x$ is the average of E_x over the illuminated volume Ω of the crystal. Thus, under these conditions, $Q(H)$ is proportional to $\alpha(H)H$. The experimental values of Q are antisymmetric for H positive and negative, and Q is linear in H at low magnetic field (the low field Hall effect). A departure from linearity becomes apparent at high fields as the temperature is reduced and the mobility increases.

An alternative procedure, particularly useful for the low field Hall mobility, is to employ the detector as a null device by adjusting the ground tap an amount ΔV to give zero indication in the presence of a magnetic field. This condition is expressed by

$$Q(H)=\int_{\text{Vol}}\left\{\sigma(H)\left[E_y+\frac{\Delta V}{D}\right]-\alpha(H)HE_x\right\}\frac{\tau_t}{D}d\mathbf{r}=0. \quad (6)$$

A balance is obtained first for H positive and then for H negative. An equation similar to (6) is obtained for H negative and can be subtracted from Eq. (6). Using the fact that the coefficients $\sigma(H)$ and $\alpha(H)$ are even in H, one obtains an expression for $\Delta V_T\equiv\Delta V(+)-\Delta V(-)$, as follows:

$$\Delta V_T=\frac{2D\alpha(H)}{\sigma(H)}H\bar{E}_x. \quad (7)$$

Therefore, the quantity ΔV_T depends upon $\alpha(H)/\sigma(H)$. At low values of $\omega\tau=\mu H/c$, ΔV_T is proportional to the Hall angle.[8]

III. EXPERIMENTAL RESULTS

A. Transient Photoconductivity

In general, the photoconductivity results for AgBr were very similar to those obtained for AgCl as reported in reference 16. The wavelength dependence of the transient photoconductivity is shown in Fig. 2 for both materials. Response begins coincident with the rise in optical absorption at 465 mμ in AgBr and at 386 mμ in AgCl. Little or no light is absorbed at longer wavelengths in each case resulting in zero induced charge and therefore no photosignal. At short wavelengths all the incident photons are absorbed. In AgBr, response with a high yield prevails through the absorption tail, through the first exciton peak, and into the second strong absorption maximum. The gradual over-all decrease at short wavelengths in the charge collected per incident photon, Q/N_0, depends in a structure-sensitive way upon preparation of the crystal surface. As explained in the case of AgCl,[16] the surface must be very carefully annealed and etched for appreciable response at large light absorption constants.

Saturation curves of the type shown in Fig. 4 of reference 16 can be obtained for AgBr. This permits evaluation of the electron range before trapping and also quantum efficiency (electron yield per photon absorbed). At the wavelength of maximum photoresponse (440 mμ at 80°K) in AgBr, the quantum efficiency was of the order of 0.6, which again is similar to the case of AgCl. Although the photoconductivity decreases markedly as the temperature is lowered to 6°K, this is apparently due to a decrease in electron lifetime (before trapping) and not to a decrease in yield. The photoresponse in the best zone refined AgBr sample was considerably higher at 6°K than that in AgCl at this temperature. The position of the absorp-

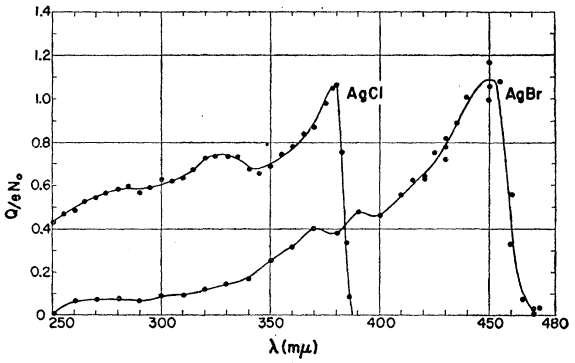

FIG. 2. Transient photoresponse per incident photon as a function of wavelength for AgCl and AgBr. The measurements were taken by the method described in reference 16 (forward polarity). The vertical scale is arbitrary in the sense that a different electric field was used for each crystal.

tion edge shifts slightly to shorter wavelengths as the temperature is lowered, in agreement with the data of Okamoto.[20]

In order to detect charge flow due to holes alone, it is necessary to use strongly absorbed light and to apply a positive voltage at the transparent electrode, thus causing positive carriers to drift into the crystal. The charge Q, as measured by the electrometer, will increase linearly with applied voltage for an unsaturated contribution by holes. Spurious effects such as those due to space charge and to nonequipotential surfaces can be eliminated. Holes were not observed to drift in AgCl at low temperature,[16] but they do appear to make a small contribution to the photocurrents in AgBr.

One sample of AgBr crystal Z-15.2 showed particularly large carrier ranges. This crystal was cut from near the center of an ingot zone-refined in vacuum. Incident light pulses of 300 mμ wavelength were used. The absorption constant for this wavelength is about 6×10^4 cm^{-1} at 80°K and 2×10^4 cm^{-1} at 10°K.[20] Figure 3 shows the response Q/N_0 in arbitrary units for both forward (electron) and reverse (hole) polarity as a function of temperature. Notice that the response for both polarities decreases sharply at low temperature. There is evidence that part of this is due to surface effects. The unit range of electrons, $w_0=w/E$, where E is electric field, was obtained from saturation curves for Z-15.2 at 80°K for two different wavelengths, as shown in Table I. Theoretical saturation curves were used taking proper account of light absorption depth. The wavelengths 465 and 420 mμ were chosen to give volume and surface release of charge, respectively. Roughly the same w_0 was obtained in each case.

The presence of shallow traps in AgBr was confirmed by the observation of electrical glow peaks.[16] Crystal Z-23.9 was illuminated at 6°K, then warmed at a rate of 0.02 to 0.08 deg/sec. Carriers were released upon warming, resulting in current peaks at 16.6, 42, and 136°K.

The electron range for a sample Z-23.9 cut near one end of the zone-refined ingot, is also given in Table I along with values for Z-15.2 and for AgCl. Notice that

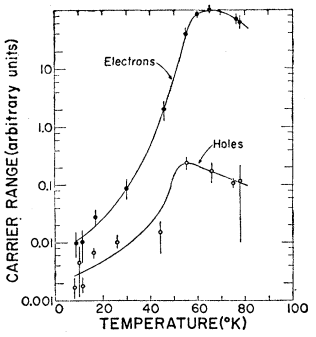

FIG. 3. Transient photoresponse as a function of temperature for forward (electrons) and reverse polarity (holes) in AgBr. The yield of electrons per absorbed photon is assumed to be approximately constant; therefore, the vertical scale is proportional to carrier range.

[20] Y. Okamoto, Nachr. Akad. Wiss. Göttingen, Math. physik. Kl. IIa, No. 14, 275 (1956).

TABLE I. Unit range of electrons at 80°K as deduced from saturation curve measurements.[a]

Crystal	Wavelength used (mμ)	Absorp. constant (cm^{-1})	Electron range (cm^2/volt)
AgBr Z-15.2	465	10^{-3}	1.03×10^{-4}
AgBr Z-15.2	420	180	1.55×10^{-4}
AgBr Z-23.9	420	180	$(9\pm1)\times10^{-6}$
AgCl XIX$_4$ (vac. grown)	240–380	···	1.5×10^{-6}
AgCl XXII$_4$ (air grown)	340	900	1.05×10^{-3}

[a] Data for AgCl is taken from reference 16.

the range in Z-15.2 is remarkably long for an unsensitized[12,21] crystal grown in an inert atmosphere or vacuum. It compares with the long range found for air-grown crystals of AgCl.

The reverse polarity response was quite small in all crystals and, in fact, was only observable at collecting voltages above 600 volts for a crystal 1.7 mm thick. (Forward polarity response due to electron drift could be observed for applied potentials as low as 5 volts.) The reverse-polarity signal was opposite in sign from the small zero field response due to Dember effect[22]; furthermore, it increased with applied voltage. It does not seem reasonable to ascribe the reverse polarity signal to ambipolar diffusion and dissociation or other extraneous effects. Therefore, we will tentatively assign the reverse-polarity response to mobile holes in the temperature range 40 to 80°K. The relative range of electrons to holes at 80°K was $w_e/w_h=400\pm60$.[23]

Figure 3 shows that the range of holes drops suddenly below 40°K, probably because of trapping. In fact, it is not clear that the very small reverse polarity signal at 10°K arises because of the drift of holes at all. The light penetration depth at this temperature is about $(1/K)=6\times10^{-5}$ cm which is comparable with the range of electrons at high field. Therefore, we assume, with only slight reservations, that the contribution of holes is negligible in Hall experiments below 40°K and, because of the small relative range, certainly negligible above 40°K.

B. Hall Measurements

In actual practice, a balance point corresponding to a null signal was achieved by adjustment of a potentiometer ΔR, rather than a battery tap, as shown schematically in Fig. 1. The potentiometer setting (either side of center) is shown in Fig. 4 as a function of magnetic field for a zone-refined sample at 6°K. The symmetric S-shaped curve is in agreement with the theoretical predictions and indicates a fairly large

[21] J. W. Mitchell in *Progress in Semiconductors* (Heywood and Company, 1958), Vol. 3, p. 55.

[22] The diffusion distance of electrons in AgBr at 80°K is about 10^{-3} cm at 80°K for $w_0=10^{-4}$ cm^2/volt.

[23] Holes have been found to be mobile in AgBr at room temperature, but their Hall mobility is about 1/35 times the mobility of electrons at the same temperature. See R. C. Hanson and F. C. Brown, J. Appl. Phy. **31**, 210 (1960).

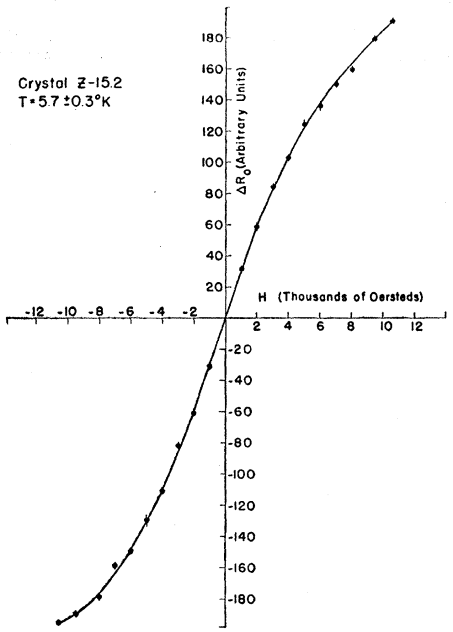

FIG. 4. Showing the adjustment for balance with positive and negative magnetic field. The quantity ΔR_0 is proportional to ΔV as explained in the text.

mobility. Departure from linearity at high magnetic fields is the result of a correction factor which is even in $\mu H/c$.

The quantity of main interest is the Hall mobility. It was determined point by point as a function of temperature by observing $\Delta R_T=\Delta R(+)-\Delta R(-)$ at low magnetic fields. Values of μ_H in cm²/volt sec were computed from

$$\frac{2\mu_H H}{c}=\frac{1}{300G}\left(\frac{l}{D}\right)\frac{\Delta R_T}{R}, \tag{8}$$

where c is the velocity of light, l the length of the resistance film, D the thickness of crystal plus spacer, H the magnitude of the magnetic field in oersteds and R the resistance of the potentiometer connected across the film. The quantity G is a numerical factor somewhat less than 1.0, computed in each case from a solution of the electrostatic field problem ($G=0.73\pm0.01$ for crystal Z-19.0 with a spacer). When appropriate, G was corrected to take account of light absorption in the sample and nonuniform release of charge. In the case of crystal Z-19.0, however, this was a negligible correction because of the use of a thick AgBr crystal and a Corning filter in the light path. (One of the following color specifications depending upon the range of temperature: 3–69, 3–70, 3–71, or 3–72.[24])

[24] These are sharp cutoff filters which pass the longer wavelengths. The zone refined crystals of AgBr showed no response at long wavelengths beyond 465 mμ. For these, a 3–69 filter could not be used. Samples such as II-222 grown from high purity but not zone-refined, material had a very small but measurable response at long wavelengths.

The low-field Hall mobility of four crystals of AgBr is shown as a function of temperature in Fig. 5. Notice that μ_H rises steeply as the temperature is lowered until approximately constant mobilities are reached below 15°K. Crystals Z-15.2 and Z-19.0 were cut from near the middle, and to the right of the middle (in the direction of zone travel), respectively, of a zone-refined ingot. Samples II-221 and 222 were cut from a Bridgman crystal grown from filtered, high purity, but not zone-refined, material. They were oriented by back-reflection x-ray patterns, so that the large faces were (100) planes. No significant differences in Hall or higher-order effects were noted which could be ascribed to orientation.

The scatter in the points (Fig. 5) is indicative of the relative accuracy of the Hall data. Balance could usually be achieved with fair precision as shown by the average deviations given in Fig. 4. The absolute mobility at a given temperature was subject to systematic errors which arose in computation of the electric field and sometimes in connection with a correction for nonuniform release of charge in the crystal. Consequently, the absolute values given in Fig. 5 are thought to be accurate to about 10%. The temperature

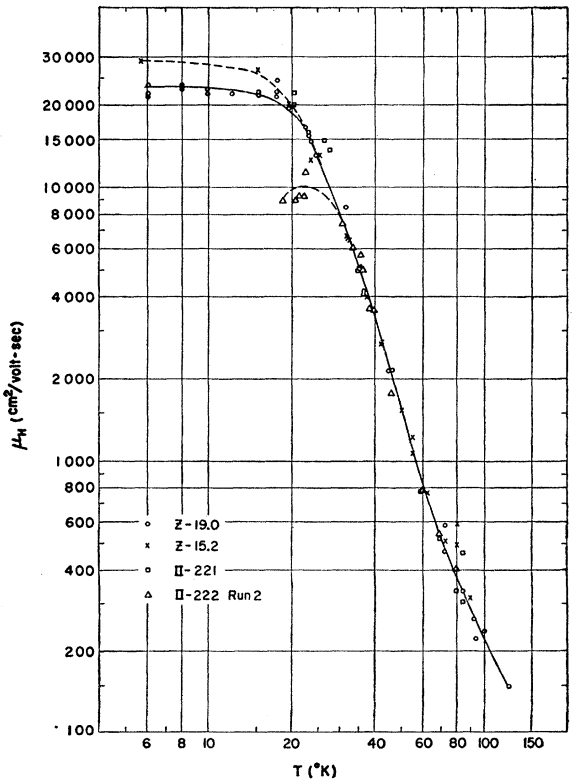

FIG. 5. Observed Hall mobility for different crystals of AgBr. The Z samples were cut from a zone refined ingot—those marked II from a crystal grown by the Bridgman technique from high purity material. The correction factor for field distribution and uniformity of range was known most accurately in the case of Z-19.0.

was known for each point with an uncertainty of $\pm 1.0°K$.

Crystal Z-19.0 was investigated using a dielectric spacer of AgCl as discussed in Sec. II and footnote 18. In this case the absolute values of low-field Hall mobility are believed to be most reliable. See Fig. 6. The dotted curves and solid line shown in this figure were drawn to compare with theory and will be discussed in Sec. IV. Notice that on this $\log\mu_H$ versus $1/T$ plot, there is a wide range of temperature over which the data fall close to a straight line.

C. High-Field Effects

As explained in Sec. II, the effects of the magnetic field can be observed in two ways. In the first of these the induced charge Q is observed as a function of H for

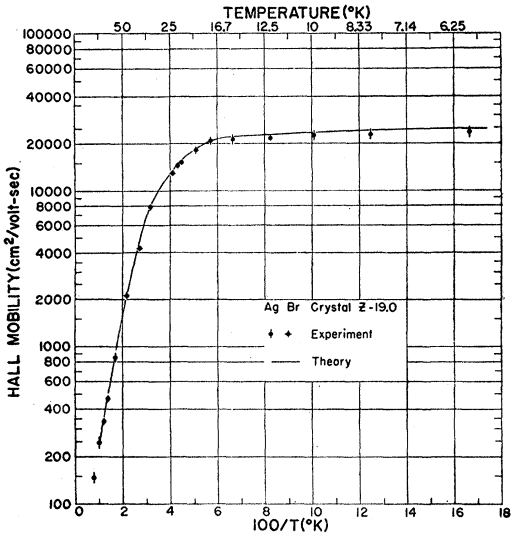

FIG. 6. Hall mobility as a function of $1/T$ for sample Z-19.0. The data is given by the points with estimated uncertainty as shown. The solid curve is computed from a proper combination of optical, acoustical and imputity scattering as described in Sec. IVA.

single light pulses of constant intensity and duration; Eq. (5) describes the expected behavior. In the second method the ground tap is varied to give zero induced charge for forward and reverse directions of H, as described by Eq. (7). The first of these methods is much more sensitive to the nonlinear effects of high magnetic field. Figure 7 shows pulse height data Q, in arbitrary units, as a function of magnetic field for crystal Z-19.0 at 31.5°K. The solid and dotted lines are drawn according to Eq. (5) and the theoretical values of the coefficient $\alpha(H)$, as discussed in the next section. The departure of these curves from straight lines indicates the importance of magnetic field terms of higher order than those involved in the low-field Hall coefficient. These nonlinear effects become increasingly important as the temperature is lowered. See Figs. 8 and 9, which give data in the vicinity of 19° and 6°K, respectively.

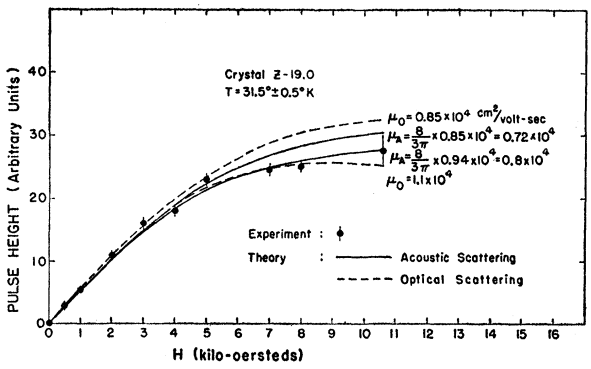

FIG. 7. The pulse-height signal is plotted as a function of magnetic field for a fixed balance obtained at $H=0$. The vertical scale depends directly on the coefficient $\alpha(H)$.

Results taken in the second manner mentioned above may be compared with Eq. (7). Less significant departures from linearity are both expected and observed at all temperatures. At 6°K the higher order effects are appreciable, however, as shown by the S-shaped curve of Fig. 4.

IV. COMPARISON WITH THEORY

A. Low Field Effects

In this section the temperature dependence of the Hall mobility is compared with theory. Various scattering mechanisms are discussed and the most plausible combination compared with experiment.

Figure 5 shows that the mobility of electrons varies very rapidly with temperatures from 40 to 125°K. It may be seen in Fig. 6 that over this temperature range the experimental points fall close to a straight line when $\log\mu_H$ is plotted at a function of $1/T$. The range is wide enough to estimate the slope of the exponential and therefore the value of the Debye Θ which enters into the theory of scattering by optical vibrations of the lattice. Since the relaxation time is independent of

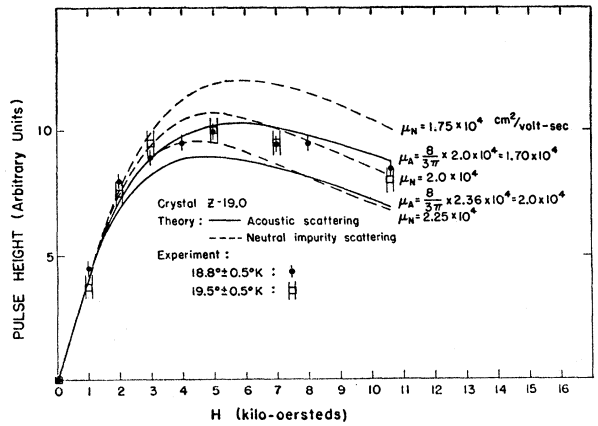

FIG. 8. Data similar to that shown in Fig. 7 but for temperatures near 19°K.

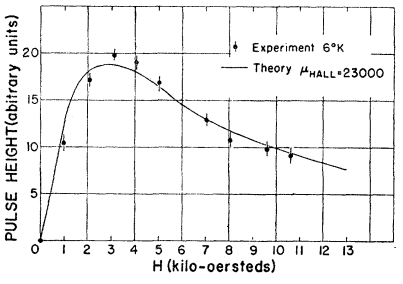

FIG. 9. Data similar to that shown in Fig. 7 but for a temperature near 6°K. Note that the high field effect has become apparent at a lower value of H. The shape of the curve is best explained by impurity scattering which is predominant at this temperature as discussed in Secs. IVA and C.

energy for optical scattering, the Hall mobility equals the drift mobility and is given by $\mu=\text{const}(e^{\Theta/T}-1)$.[4–7] From the data of Figs. 5 and 6, $\Theta=195\pm15$°K. The value of Θ computed from[25] $\omega_l=\omega_t(\epsilon_0/n^2)^{\frac{1}{2}}$ and a reststrahlen wavelength of 125μ[26] is 194°K. On the other hand, the reststrahlen data for AgCl indicates a value of $\Theta=280$°K. The difference in slope can be distinguished in the mobility data for the two materials.[8] Optical scattering and the polaron will be discussed further in Sec. IVB.

At low temperatures the optical vibrations freeze out and one or more impurity scattering mechanisms dominate. Three quite different possibilities are: scattering by neutral impurities, by dipoles of atomic dimension, and by isolated charges. The first of these, neutral scattering, has been discussed for semiconductors by Erginsoy[27] on the basis of a hydrogen atom model. The scattering is weak; concentrations of 10^{17} to 10^{18} cm^{-3} appropriate impurities would have to be present. Imperfections which fit the hydrogen atom model are probably not so prevalent in AgBr. For example, Schottky disorder is negligible in the silver halides and the small number of negative ion vacancies limits the concentration of F centers which can be formed. In addition, arguments having to do with the observed high field effects are given in Sec. IVC which tend to reject neutral scattering as a possibility.

A center which would fit the dipole model for these crystals might consist of a divalent substitutional impurity and an associated vacancy, i.e., a complex. According to Blatt[28] a dipole of atomic dimension would be about 10^{-3} times as effective a scattering center as an isolated charge. Charged defects such as unassociated impurity ions would have to be present in correspondingly small numbers for scattering by complexes to dominate. This does not appear entirely reasonable. For example, Tucker[29] has shown by spin resonance experiments that an appreciable fraction of substitutional Cu^{++} ions in AgCl remain unassociated even after slow cooling to low temperatures..

It would seem as if the most important scattering centers at low temperature are charged defects such as impurity ions and oppositely charged vacancies (or alternatively impurity ions of both sign) present in equal numbers throughout the crystal. The statement that positive and negative defects are present in equal numbers, which guarantees neutrality without the presence of free carriers or trapped charge, means that distant impurity ions are effectively screened. This and the fact that the scattering centers are widely separated in the crystal points toward the use of the theory of Conwell and Weisskopf.[30] Their formula for scattering time is valid for impurity concentrations around $N_i=2\times10^{14}$ cm^{-3} or less and temperatures down to 10°K.[31] For lower temperatures and higher concentrations, an improvement on the classical calculation can be made by the use of the partial wave method,[32] but this is not thought worthwhile for the present data.

As a first attempt, the data of Fig. 6 can be compared with theory using a combination of optical scattering (predominant at high temperatures) with charged impurity scattering (predominant at low temperatures). The amount of each scattering can be adjusted for a good fit of the data at extreme temperatures, but the result of the combined scattering is a very poor fit at intermediate temperatures (15 to 30°K). An additional mechanism such as scattering by acoustical vibrations of the lattice is required. Although the number of samples studied is limited, there is evidence that this additional scattering is intrinsic and not structure dependent. Also, a choice of a certain amount of acoustic scattering will be in agreement with the higher order effects discussed in Sec. IVC.

A proper combination of optical, acoustical and charged impurity scattering has been made using the graphical results of Porfir'eva,[33] as well as the integrals tabulated by Dingle *et al.*[34] The combined probability of scattering is given by

$$\frac{1}{\tau}=\frac{1}{\tau_0}+\frac{1}{\tau_a}+\frac{1}{\tau_i}. \tag{9}$$

A single effective mass and isotropic scattering is implicit in our discussion of the various scattering probabilities.

[25] R. H. Lyddane, R. G. Sachs, and E. Teller, Phys. Rev. **59**, 673 (1941).
[26] R. B. Barnes, Z. Physik **75**, 723 (1932).
[27] C. Erginsoy, Phys. Rev. **79**, 1013 (1950).
[28] F. J. Blatt (private communication).
[29] R. F. Tucker, Phys. Rev. **112**, 725 (1958).
[30] E. Conwell and V. F. Weisskopf, Phys. Rev. **77**, 388 (1950).
[31] The situation corresponds to $n=N_I$ so that the Brooks-Herring formulation gives nearly the same numerical results as the Conwell-Weisskopf expression. See P. P. Debye and E. M. Conwell, Phys. Rev. **93**, 693 (1954).
[32] F. J. Blatt, in *Solid State Physics*, edited by F. Seitz and D. Turnbull (Academic Press, Inc., New York, 1956).
[33] N. N. Porfir'eva, Soviet Phys. Solid-State Phys. **1**, 794 (1959).
[34] R. B. Dingle, D. Arndt and S. K. Roy, Appl. Phys. Sci. Research **B6**, 144, 245 (1956).

According to the theory of scattering by optical mode vibrations[4–7]

$$\tau_0 = C(e^{\Theta/T}-1), \tag{10}$$

where C is a constant, independent of temperature, but given in various ways by the different polaron theories in terms of the (unknown) effective mass of the electrons. For AgBr $\exp\Theta/T$ becomes large compared with unity below about 80°K. The value of C in Eq. (10) is chosen so that $\mu_H=(e/m)\tau_0=37(e^{195/T}-1)$ cm²/volt-sec which best fits the experimental data for μ_H at high temperatures where optical scattering dominates. A small adjustment is made for best fit at intermediate temperatures after the approximate amount of acoustical and impurity scattering is known. The Debye temperature Θ is taken to be 195°K as discussed in the first paragraph of this section.

A complete discussion of scattering by acoustic vibrations in a polar crystal has not been given. However, for a cubic crystal such as AgBr it seems reasonable as a first attempt to adopt the usual deformation potential theory,[35] according to which τ_a is of the form

$$\tau_a=\left[\frac{\pi\hbar^4 c_{ii}}{\sqrt{2}m^{\frac{3}{2}}E_1^2}\right]\frac{x^{-\frac{1}{2}}}{(\kappa T)^{\frac{3}{2}}}, \tag{11}$$

where $x=\epsilon/\kappa T$, κ is Boltzmann's constant, m is the effective mass of the electrons, ϵ their energy, c_{ii} is an appropriate elastic constant for a longitudinal wave in the crystal, and E_1 is the deformation potential proportionality constant for the conduction band. The quantity in square brackets is not well known and so will be determined empirically for a best fit to the data at a temperature $T=20$°K. For this purpose the amount of impurity scattering must be ascertained, and this is feasible at extremely low temperatures, $T\approx 6$°K, where even acoustic lattice scattering is nearly frozen out.

The Conwell-Weisskopf formula for τ_i is[30]

$$\tau_i=\frac{\sqrt{2}m^{\frac{1}{2}}\epsilon_0^2(\kappa T)^{\frac{3}{2}}x^{\frac{3}{2}}}{\pi N_i e^4\ln(1+9\epsilon_0^2\kappa^2T^2/e^4N_i^{\frac{2}{3}})}. \tag{12}$$

Here we have replaced electron energy in the slowly varying ln term by an average $\epsilon=3\kappa T$. Again m, and N_i, the concentration of charged centers, are uncertain, so that we choose the coefficient of $x^{\frac{3}{2}}$ to best fit the data at 6°K.[36] Using a trial amount of impurity scattering and knowing the temperature dependence of each mechanism, one can normalize at 20°K by adjusting the amount of acoustic interaction.

In carrying out the curve fitting procedure, the Hall mobility at low fields is used as follows:

$$\mu_H=\frac{e}{m}\frac{\langle\tau^2\rangle}{\langle\tau\rangle}, \tag{13}$$

where the brackets indicate the usual average over the Boltzmann distribution [Eq. (3.71) of reference 32]. Following Porfir'eva[33] μ_H can be written in terms of a function $Y(A,I)$:

$$\mu_H=(e/m)\tau_0 Y(A,I), \tag{14}$$

where $A=(\tau_0/\tau_a)x^{-\frac{1}{2}}$ measures the amount of acoustical scattering relative to optical scattering and $I=(\tau_0/\tau_i)x^{\frac{3}{2}}$ the corresponding relative amount of impurity scattering. The quantity $Y(A,I)$ is given by $G(A,I)/F(A,I)$, where

$$F(A,I)=\left\langle\frac{1}{1+Ax^{\frac{1}{2}}+Ix^{-\frac{3}{2}}}\right\rangle,$$

and

$$G(A,I)=\left\langle\frac{1}{(1+Ax^{\frac{1}{2}}+Ix^{-\frac{3}{2}})^2}\right\rangle. \tag{15}$$

The graphical results of reference 33 may be used for computing $Y(A,I)$ in the range of temperatures where three mechanisms must be included. On the other hand, at low temperatures where the optical interaction is frozen out, the problem can be reformulated in terms of the ratio I/A by utilizing the functions $\mathfrak{D}_{9/2}$ and $\mathfrak{E}_3$ of reference 34. The parameter I/A depends upon temperature and measures the amount of impurity scattering relative to acoustic scattering.

The result of combining the different scattering processes as outlined is shown as a solid curve in Fig. 6. For this curve the scattering times are given in cgs units by

$$\begin{aligned}&(e/m)\tau_0=1.11\times10^4(e^{195/T}-1),\\&(e/m)\tau_a=2.73\times10^{-15}/(\kappa T)^{\frac{3}{2}}x^{\frac{1}{2}},\\&(e/m)\tau_i=9.36\times10^{28}(\kappa T)^{\frac{3}{2}}x^{\frac{3}{2}}/\ln(1+0.142T^2).\end{aligned} \tag{16}$$

Values of N_i and E_1 can be estimated on the basis of Eqs. (11), (12), and (16) if we assume $m=m_e$. The result for N_i is $N_i=2.46\pm0.05\times10^{14}$ cm^{-3}, which is a reasonable fraction of the total heavy metal content determined spectrographically. Setting $c_{ii}\approx c_{11}=5.6\times10^{11}$ for AgBr,[37] $m=m_e$, and using Eq. (11), the energy E_1 comes out to be about 2.0 ev, which also seems reasonable. It may well be that acoustical scattering arises because of the polarization associated with these vibrations when oppositely charged ions are not the same mass. This can be distinguished from deformation potential scattering but it has the same dependence on energy and temperature as Eq. (11). One obtains a value of $(e/m^*)\tau_u'$ very close to $(e/m)\tau_a$ given in Eq. (16) by using the formula of Meijer and

[35] J. Bardeen and W. Shockley, Phys. Rev. **80**, 72 (1950).

[36] To actually determine N_i in this way the effective mass must be known. The latter is chosen to be equal to the free electron mass when picking N_i for use in the ln term—an approximation which should introduce only a small error.

[37] D. Tannhauser and A. Lawson, J. Chem. Phys. **22**, 2092 (1954).

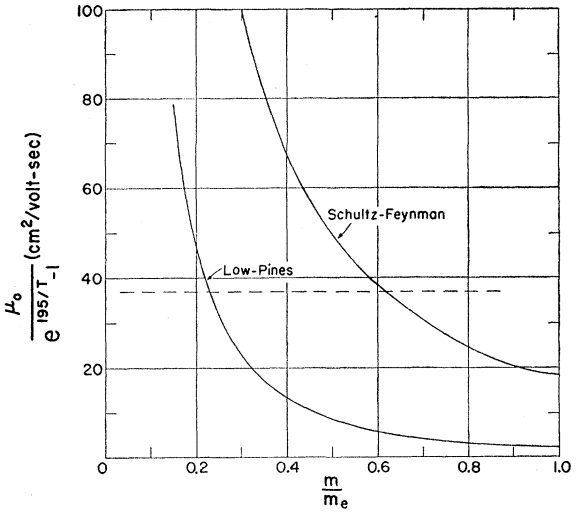

FIG. 10. Mobility computed from polaron theory as a function of the ratio of bare electron effective mass to free electron mass. The experimental value from the data of Fig. 6 is shown as a horizontal dotted line.

Polder,[37a] an effective charge $e^*/e=0.73$ and $m^*/m=0.3$. (See Sec. IVB).

Although the assignment of impurity scattering as explained above is tentative, pending further work on doped crystals, the agreement with the shape of the experimental data is remarkable. Further support for the choice of impurity scattering predominant below 10°K is given in Sec. IVC. The observation that Hall mobility levels off to a nearly constant value at low temperature has been made in the case of other ionic crystals.[9] It seems to be a result of the combination of optical, acoustical and impurity scattering (as explained above) and of the way in which the average over energy is made for the combined scattering.[37b]

B. Optical Scattering and Polaron Theory

The optical mode scattering seems to be sufficiently clear in AgBr to warrant a comparison with polaron theory. The Debye $\Theta=195$°K as well as considerations involving the validity of the Boltzmann equation[7] place an upper temperature limit on the validity of the theory, but there still seems to be a useful region for comparison before impurity or acoustical interaction sets in at low temperatures.

For purposes of discussion, a choice can be made between the intermediate coupling theory[6] or the more recent approach of Schultz[7] based on a model by Feynman. In both cases the usual coupling constant α is a measure of the strength of interaction of the electron with the lattice. The Debye Θ for AgBr corresponds to a vibrational frequency of $\omega_l=2.54\times10^{13}$ sec^{-1}. From this and the dielectric constants ($\epsilon_0=13.1$, $n^2=4.62$) it turns out that $\alpha=4.0(m/m_e)^{\frac{1}{2}}$, where (m/m_e) is the ratio of the effective mass of the bare conduction electron to the free electron mass. This ratio is unknown and enters as a parameter in the mobility expressions; it might be obtained by comparison with the mobility data, but, as shown below, the two theories depend upon the effective mass in different ways.

In one case the mobility is given by Eq. (6.1) of reference 8 which contains the resonance velocity v_r and coupling renormalization Z_r, each a function of α (see Table IV, reference 8). By interpolating this tabulated quantity graphically, the mobility μ can be plotted in terms of m/m_e. A similar procedure can be carried out in the case of the mobility formula of Low and Pines.[6] The results for the two theories are shown as solid lines in Fig. 10. The dotted line indicates the experimental value of $\mu_0/(e^{195/T}-1)$ as discussed in Sec. IVA. It is seen that widely different effective masses result in the two cases. According to Schultz, m/m_e is about 0.62 which results in a coupling constant $\alpha=3.2$ and a zeroth-order polaron mass of about $m_0=1.1m_e$. On the other hand, the Low-Pines expression gives $m/m_e=0.23$, $\alpha=1.9$, and a polaron mass $m^*=(1+\frac{1}{6}\alpha)m=0.31m_e$.

The two results are sufficiently different that it might be possible to distinguish between them from an independent measurement of effective mass perhaps by a cyclotron resonance experiment. Such an experiment would be just possible with existing techniques ($\omega\tau=\mu H/c\approx2.0$ for $H=10^4$ at 6°K). It would not provide a detailed check on polaron theory since it would measure only the polaron mass and not the ratio m^*/m. However, the polaron effect is sufficiently different in the two theories that independent information such as provided by cyclotron resonance would be most interesting.

C. High-Field Effects for Separate Scattering Mechanisms

The functions σ, α, and γ introduced in Sec. II can be obtained in closed form on the following simple model. It is assumed that conduction occurs primarily in a single band of standard form, i.e., that the energy-

TABLE II. Relationship between the conductivity, Hall, and magnetoresistance functions [Eq. (20)] and the tabulated functions $\mathfrak{A}_p(x)$ and $\mathfrak{E}_n(x)$ of Dingle, Arndt, and Roy.[a] Here $z=\omega\tau_c=[(\frac{3}{2})!/(p+\frac{3}{2})!](\mu H/c)$.

	$p=-\frac{1}{2}$	$p=0$	$p=\frac{1}{2}$	$p=\frac{3}{2}$
$\sigma(H)/\sigma(0)$	$2\mathfrak{A}_2(z^2)$	$(1+z^2)^{-1}$	$z^{-2}\mathfrak{A}_2(z^{-2})$	$\mathfrak{E}_3(z^2)$
$\alpha(H)/\alpha(0)$	$\frac{3}{2}\mathfrak{A}_{3/2}(z^2)$	$(1+z^2)^{-1}$	$z^{-2}\mathfrak{A}_{5/2}(z^{-2})$	$\mathfrak{E}_{9/2}(z^2)$
$\gamma(H)/\gamma(0)$	$\mathfrak{A}_1(z^2)$	$(1+z^2)^{-1}$	$z^{-2}\mathfrak{A}_3(z^{-2})$	$\mathfrak{E}_6(z^2)$

[a] See reference 34.

[37a] H. J. Meijer and D. Polder, Physica **19**, 255 (1953).

[37b] This last statement is reasonable for AgBr, however a difficulty arises in those cases (alkali halides) where the trapping time is very short. More information is needed on the relative cross sections for scattering and for trapping at low temperatures in these crystals.

momentum relationship for the carriers is

$$\epsilon(k)=\hbar^2\mathbf{k}^2/2m, \tag{17}$$

that a meaningful relaxation time $\tau(\mathbf{k})$ exists, and that the carrier distribution function obeys the classical steady-state Boltzmann equation[38]

$$\frac{e}{\hbar}\left[\mathbf{E}+\frac{1}{c}(\mathbf{v}\times\mathbf{H})\right]\cdot\nabla_k f=-\frac{f-f_0}{\tau(\mathbf{k})}. \tag{18}$$

We use the equilibrium distribution for nondegenerate statistics, $f_0(\epsilon)=C\exp(-\epsilon/\kappa T)$, where κ is Boltzmann's constant and $C=4\pi^3\hbar^3 n_0(2\pi m\kappa T)^{-\frac{3}{2}}$ is a normalizing factor involving the density of carriers n_0. The relaxation time is assumed to have the form

$$\tau=\tau_c(\epsilon/\kappa T)^p=\tau_c x^p. \tag{19}$$

When now the distribution function and the current density $\mathbf{J}$ are expanded in powers of E, the linear part of $\mathbf{J}$ is readily found[39] to have the form of Eq. (2), with

$$\sigma(H)=n_0e\mu\left[\frac{1}{(p+\frac{3}{2})!}\int_0^\infty\frac{x^{p+\frac{3}{2}}e^{-x}}{1+\omega^2\tau_c^2x^{2p}}dx\right],$$

$$\alpha(H)=n_0e\mu\frac{\mu_H}{c}\left[\frac{1}{(2p+\frac{3}{2})!}\int_0^\infty\frac{x^{2p+\frac{3}{2}}e^{-x}}{1+\omega^2\tau_c^2x^{2p}}dx\right], \tag{20}$$

and

$$\gamma(H)=n_0e\mu\frac{\mu_H\mu_H'}{c^2}\left[\frac{1}{(3p+\frac{3}{2})!}\int_0^\infty\frac{x^{3p+\frac{3}{2}}e^{-x}}{1+\omega^2\tau_c^2x^{2p}}dx\right].$$

Here ω is the circular cyclotron resonance frequency eH/mc, μ is the zero-field drift mobility

$$\mu=(e/m)\tau_c[(p+\tfrac{3}{2})!/(\tfrac{3}{2})!], \tag{21}$$

and μ_H is the Hall mobility

$$\mu_H=\{(\tfrac{3}{2})!(2p+\tfrac{3}{2})!/[(p+\tfrac{3}{2})!]^2\}\mu. \tag{22}$$

μ_H' is not used again in this paper; it may be obtained from Eq. (22) by making the following replacements: $\mu_H\rightarrow\mu_H'$, $\mu\rightarrow\mu_H$, $\frac{3}{2}\rightarrow\frac{3}{2}+p$.

For $\omega\tau_c x^p\ll 1$, it is possible to expand the integrands in (20) formally in powers of ω^2 (i.e., in H^2), and the results are equivalent to an iterative solution of the Boltzmann equation as carried out by Seitz[40] and by Blatt.[32] For example, when $p=-\frac{1}{2}$,

$$\begin{aligned}\sigma&\approx n_0e\mu(1-\omega^2\tau_c^2),\\ \alpha&\approx n_0e\mu(\mu_H/c)(1-2\omega^2\tau_c^2).\end{aligned} \tag{23}$$

These expressions correspond to Seitz's $\sigma_0+\beta H^2$ and $\alpha+\epsilon' H^2$, respectively.[41] Kobayashi and Brown[8] have used Seitz's notation in their analysis of the Hall effect in AgCl.

The functions (20) are even functions of $\omega\tau_c$ (and, therefore, of $\mu H/c$) and the quantities in square brackets are unity at $\omega=0$. We therefore denote the coefficients of these square brackets by $\sigma(0)$, $\alpha(0)$, and $\gamma(0)$, respectively. The integrals involved have been studied and tabulated in reference 34. Table II shows the relationship between our functions and their functions $\mathfrak{A}_p(x)$ and $\mathfrak{E}_p(x)$.

The tabulated integrals and expressions (20) have been used in conjunction with Eq. (5) to compare the simple theory with the high field experiments. For this purpose various reasonable scattering mechanisms were chosen in plotting the theoretical curves of Figs. 7, 8, and 9. For example, curves for lattice scattering by optical modes ($p=0$) and by acoustical modes ($p=-\frac{1}{2}$) are shown in Fig. 7. Different values of mobility are used to illustrate the sensitivity of the shape of the curves to this quantity. The theoretical curves are normalized to agree with experiment at low magnetic field. It is significant that by varying μ to fit the high field effects, one arrives at a value of μ_H which agrees quite well with the low field Hall mobility obtained using Eq. (8) and discussed in Sec. IVA. Note in Fig. 8 that the curves for $\mu_H=2.0\times10^4$ cm^2/volt-sec are only slightly different for $p=0$ and $p=-\frac{1}{2}$ if the difference between μ_H and μ is taken into account [i.e., $\mu_H=(3\pi/8)\mu$ for acoustic scattering but $\mu_H=\mu$ for optical or neutral impurity scattering]. The fact that a unique drift mobility can be used to explain both the low field and high field effects lends support to the assumptions used in the theory. It is interesting, for example, that the classical Boltzmann equation agrees with experiment for $\omega\tau\gtrsim 1$ ($H\gtrsim 8000$ oersteds).

Although the different scattering mechanisms cannot be deduced with certainty from the high field effects alone some information can be obtained. If one is willing to ascribe the observed mobility at 30°K to lattice scattering the choice rests between optical and acoustical scattering or a combination of these. Either will fit the data of Fig. 7 fairly well for reasonable mobilibites. However, the relaxation time for optical scattering does not depend upon energy ($p=0$). Consequently, the effect described by Eq. (7) which depends upon $\alpha(H)/\sigma(H)$ should be linear in H for all H. A distinct nonlinearity in ΔV_T was observed at high fields at 30°K, which indicates at least some admixture of energy-dependent scattering, such as that provided by acoustic lattice vibrations.

At a lower temperature (Fig. 8, 19°K), the discussion

[38] After excitation by light the conduction electrons are assumed to very rapidly approach a steady distribution in velocity. The drift term in the Boltzmann equation involving $m\nabla_r f$ is neglected in the absence of temperature gradients. The slight effect of exponential absorption of light can be incorporated into the carrier density n_0.

[39] See, e.g., reference 32 or A. H. Wilson, *The Theory of Metals* (Cambridge University Press, London and New York, 1953), 2nd ed., Chap. VIII.

[40] F. Seitz, Phys. Rev. **79**, 372 (1950).

[41] A simple series in ω^2 actually does not exist for the $p=-\frac{1}{2}$ integrals, since their exact form involves error functions and exponential integrals (see A. H. Wilson, reference 39, pp. 235-6). However, their algebraic part happens to be given correctly by (23).

of Sec. IVA indicates that acoustical mode scattering is still important. Optical mode scattering is nearly frozen out at this temperature so the energy independent mechanism used for comparison has been labeled μ_N corresponding to scattering by neutral impurities.[27] Such a mechanism is at least a possibility although considerations given in Sec. IVA argue against it.

As the temperature is lowered from 19° to 6°K the mobility increases only slightly. However, as Fig. 9 indicates, the high field effect has become considerably more important. This appears to be due to the importance of impurity scattering at the lower temperature and is just the result expected from the amount of scattering chosen to fit the mobility data as discussed in Sec. IVC. The general shape of the theoretical curve in Fig. 9 is in good agreement with experiment for scattering by charged centers ($p=\frac{3}{2}$) but does not agree well in the case of acoustical scattering ($p=-\frac{1}{2}$).

PHYSICAL REVIEW VOLUME 119, NUMBER 5 SEPTEMBER 1, 1960

Properties of Some Magnetic Superconductors

R. M. Bozorth, D. D. Davis, and A. J. Williams
Bell Telephone Laboratories, Murray Hill, New Jersey

(Received April 25, 1960)

Two solid solutions in the system $GdRu_2-CeRu_2$, in which both ferromagnetism and superconductivity have been observed, are studied by magnetic methods. The solid solution $Gd_{0.082}Ce_{0.918}Ru_2$, which has a Curie point θ above the critical temperature T_s for superconductivity, is both ferromagnetic and superconducting. In $Gd_{0.04}Ce_{0.96}Ru_2$, for which the expected $\theta<T_s$, no ferromagnetic moment could be measured, although a small moment may be present and not detected by our methods. In solid solutions of increasing Gd content, when θ begins to exceed the expected T_s by a considerable margin, T_s suddenly drops toward zero; and when $T_s>\theta$, θ approaches zero. Similar conclusions apply to the system $GdOs_2-LaOs_2$ when θ and T_s are related in the same ways. Both major and minor hysteresis loops have forms not previously observed and enable one to detect ferromagnetism and superconductivity when they exist. The molecular fields resulting from the interaction between Gd atoms, and the Curie points calculated therefrom by molecular field theory, increase with increasing temperature; this is in accordance with the theory of long-range exchange forces developed by Brout.

SUPERCONDUCTIVITY and ferromagnetism have been studied in a number of metallic compound systems by Matthias, Suhl, and Corenzwit.[1] The present paper reports more detailed studies of solid solutions in the system $CeRu_2$-$GdRu_2$ and of some other materials. The purpose of the work[2] has been to find out if superconducting materials can become ferromagnetic and if ferromagnetic materials can be superconducting at the same time, and more generally to know the influence of the one property on the other.

EXPERIMENTAL METHOD

Measurements have been made of magnetic moment as dependent on field strength H, and temperature T, over the range $H=0$ to 12 000 oe, $T=1.3$ to 300°K. Moments were usually measured by a null method using a pendulum magnetometer supporting the specimen in a field gradient, with strain gauge sensing elements, as previously described.[3] On some occasions the material was surrounded by a search coil, the field reversed (or the the sample and coil rotated 180°) and a galvanometer deflection noted. Hysteresis loops were measured using the pendulum magnetometer in a carefully calibrated electromagnet, taking into account the nonlinearity and hysteresis of the magnet and in some cases the field produced at the specimen by the current through the balancing coil, which annuls the moment of the specimen. The initial magnetization curves were measured after cooling from a sufficiently high temperature in zero field.

The materials were prepared by melting in the argon arc. X-ray examination showed them to be true solid solutions with, in some cases, a trace of uncombined ruthenium.

The specimens, having usually a dimensional ratio of about 4, were mounted at the center of the balancing coil. The sensitivity of the pendulum magnetometer was about 0.004 cgs unit in high fields, the largest moment measureable being about 40. Since the gradient was approximately proportional to the field strength, the sensitivity decreased with the decreasing field to zero at $H=0$ and measurements were not usually made with this method when $H<50$ oe; in measuring hysteresis loops the moment in zero field could be obtained by interpolating between the points for $H=\pm 50$.

[1] B. T. Matthias, H. Suhl, and E. Corenzwit, Phys. Rev. Letters **1**, 449 (1958).
[2] For a brief report of part of this work see J. Appl. Phys. **31**, 235 (1960).
[3] R. M. Bozorth, H. J. Williams, and D. E. Walsh, Phys. Rev. **103**, 572 (1956); R. M. Bozorth and D. D. Davis, Phys. Rev. **118**, 1543 (1960).